

Article

A Pairwise SSD Fingerprinting Method of Smartphone Indoor Localization for Enhanced Usability

Fan Yang ^{1,2} , Jian Xiong ³, Jingbin Liu ^{1,4,*}, Changqing Wang ², Zheng Li ¹ and Pengfei Tong ¹ and Ruizhi Chen ^{1,4} 

- ¹ State Key Laboratory of Information Engineering in Surveying, Mapping and Remote Sensing, Wuhan University, Wuhan 430079, China; fanyang1990@foxmail.com (F.Y.); 2016206440005@whu.edu.cn (Z.L.); tongpfgiser@163.com (P.T.); ruizhi.chen@whu.edu.cn (R.C.)
 - ² State Key Laboratory of Geodesy and Earth's Geodynamics, Chinese Academy of Sciences, Wuhan 430079, China; whiggskd@asch.whigg.ac.cn
 - ³ Wuhan GeoTechnical Engineering and Surveying Co. Ltd., Wuhan 430079, China; tz@hbaa.cn
 - ⁴ Collaborative Innovation Center of Geospatial Technology, Wuhan University, Wuhan 430079, China
- * Correspondence: jingbin.liu@whu.edu.cn; Tel.: +86-139-7108-2735

Received: 18 January 2019; Accepted: 3 March 2019; Published: 8 March 2019



Abstract: Smartphone indoor localization has attracted considerable attention over the past decade because of the considerable business potential in terms of indoor navigation and location-based services. In particular, Wi-Fi RSS (received signal strength) fingerprinting for indoor localization has received significant attention in the industry, for its advantage of freely using off-the-shelf APs (access points). However, RSS measured by heterogeneous mobile devices is generally biased due to the variety of embedded hardware, leading to a systematical mismatch between online measures and the pre-established radio maps. Additionally, the fingerprinting method based on a single RSS measurement usually suffers from signal fluctuations due to environmental changes or human body blockage, leading to possible large localization errors. In this context, this study proposes a space-constrained pairwise signal strength differences (PSSD) strategy to improve Wi-Fi fingerprinting reliability, and mitigate the effect of hardware bias of different smartphone devices on positioning accuracy without requiring a calibration process. With the efforts of these two aspects, the proposed solution enhances the usability of Wi-Fi fingerprint positioning. The PSSD approach consists of two critical operations in constructing particular fingerprints. First, we construct the signal strength difference (SSD) radio map of the area of interest, which uses the RSS differences between APs to minimize the device-dependent effect. Then, the pairwise RSS fingerprints are constructed by leveraging the time-series RSS measurements and potential spatial topology of pedestrian locations of these measurement epochs, and consequently reducing possible large positioning errors. To verify the proposed PSSD method, we carry out extensive experiments with various Android smartphones in a campus building. In the case of heterogeneous devices, the experimental results demonstrate that PSSD fingerprinting achieves a mean error $\sim 20\%$ less than conventional RSS fingerprinting. In addition, PSSD fingerprinting achieves a 90-percentile accuracy of no greater than 5.5 m across the tested heterogeneous smartphones

Keywords: indoor localization; smartphone navigation; received signal strength (RSS); pedestrian dead reckoning (PDR)

1. Introduction

Because of the popularity of built-in global navigation satellite systems (GNSSs) with smartphones, smartphone navigation has been one of the most popular applications. Smartphone navigation not only facilitates daily mobility by providing routing navigation from place A to place B; it also becomes a major data source for big data analysis in urban intelligent transportation. However, GNSS does not work in indoor spaces, where indoor navigation and location-based services (LBS) have considerably more business potential than current GNSS navigation outdoors [1–3]. Therefore, smartphone indoor localization has attracted considerable study efforts in the past decade to provide a smartphone with the capability of indoor localization, and a variety of solutions have been presented in the literature [4–6]. Signals of opportunity-based solutions, such as Wi-Fi fingerprinting, have been studied largely in the context of smartphone applications because of the advantages of low cost and the requirement of no additional infrastructure. Unfortunately, few of these reported solutions have been applied widely in real marketing due to several issues regarding the usability. These studies focused on the localization accuracy, while the usability was neglected. For smartphone mass users, usability is important for user experience and applicability of the solution, and therefore, usability must be considered in particular in the algorithm design.

Previous work has proposed many approaches to realize Wi-Fi indoor localization, of which fingerprinting based on received signal strength (RSS) has attracted the most attention because no prior knowledge of infrastructure position is needed compared to the traditional geometric methods [7]. Moreover, the high requirement of hardware ensuring precise ranging and a particular radio attenuation model specified for the indoor environment make the geometric method less applicable [8]. The philosophy behind the RSS-based fingerprinting approach is to first collect fingerprints in terms of RSS signatures labeled with the corresponding coordinates at a database for the offline training phase. Then, for the online phase, the user's location can be determined with the best-fitted fingerprint by comparing the measured RSS against the prebuilt database [9]. When only Wi-Fi is considered to be the location source, past work reports that either deterministic algorithms such as K-nearest neighbor (KNN) [10] or the probability (Bayesian) algorithm [9,11] in terms of RSS fingerprint expects to locate the user/device at a precision of approximately 5 m for many instances [12]. However, the following challenges remain in terms of usability:

- The heterogeneity of devices. For most of the cases, the assumption of the RSS fingerprinting method is that the devices collecting RSSI for both the offline training phase and the online phase are identical or homogeneous; otherwise, the localization accuracy is significantly degraded. This is because the RSS is influenced by a particular transmitter-receiver pair's hardware-specific parameters, such as antenna gains [13]. To overcome this, Haeberlen [14] and Kjærgaard [15] proposed a precalibration method to translate the RSS of heterogeneous devices into the benchmark device by a set of conversion formulae. However, the formulae must be found and validated in the lab in advance, which is impractical and time-consuming with the increasing number of new mobile devices. Therefore, developing a free-calibration method to reduce effects caused by heterogeneous mobile devices is a challenge towards the goal of ~5 m location precision.
- The reliability of positioning. This great challenge is the result of the large errors in RSS fingerprinting localization due to the signal fluctuations caused by many factors, i.e., the time-varying environments or body blockages [16]. The large errors usually manifest as a large gap between current Wi-Fi prediction and the previous prediction, which is apparently unreasonable because a pedestrian's historic walk track should be continuous. Some of the past works attempted to reduce the signal fluctuations regarding one or two aspects [17], but currently, there is no single universal solution for all cases. In addition, another direction is to leverage the relatively stable external sources in a fusion frame, typically, the PDR (pedestrian dead reckoning) derived information including the pedestrian's heading and walking distance [18,19]. With a deliberately designed filter, the fusion can smooth the sequence of Wi-Fi positioning and minimize

the large errors. However, frequent erroneous Wi-Fi positioning will undermine the filtering. Hence, it is still necessary to enhance the reliability of Wi-Fi positioning. How to design a pure Wi-Fi positioning system by increasing the diversity of fingerprints to further reduce large errors is a considerable challenge.

The error sources such as device differences and body blockages as well as temporal environmental changes, can be hardly avoided when fingerprinting approach is applied in reality. Rather than particular treatments with the error sources one by one, this study attempts to tolerate the errors by imposing additional spatial constraints directly in the fingerprints for the first time. To this end, we propose a pairwise signal strength difference (PSSD) indoor location system, which is extended from the traditional Wi-Fi-RSS fingerprinting method. The basic rationale behind PSSD arises from two aspects regarding the two challenges depicted. The first aspect is that the signal strength difference (SSD) that differentiates the RSS between APs is more stable than an absolute RSS value; and more importantly, the SSD is mathematically feasible for heterogeneous mobile devices. Another aspect is an introduction of spatial constraint into fingerprints by using a pairwise RSS observations to predict the pedestrian's walk track. Compared to the conventional RSS point-value positioning system, the pairwise fingerprint with user's movement information should be more robust and be less interrupted by those unavoidable error sources. Therefore, unlike several existing Wi-Fi fingerprinting approaches, the proposed PSSD actually establishes two types of fingerprint databases, SSD and pairwise RSS radio maps. In this way, our system can deal with diverse RSS measurements from heterogeneous devices and possible large errors between Wi-Fi predictions.

The paper is organized as follows. We first review the related work in Section 2. Subsequently, Section 3 details the proposed method from three aspects, the conventional SSD algorithm as well as our modification, the spatial information extraction, and finally the pairwise RSS method. In Section 4, we present and discuss the experimental results of the proposed PSSD method. Finally, we draw conclusions in Section 5 and propose future work.

2. Related Work

Wi-Fi RSS fingerprinting-based localization has been extensively studied over the past decade. Here, we only focus on the related work concerning the above two challenges.

As mentioned before, the heterogeneity of devices can significantly degrade the positioning performance of RSS-based fingerprinting. Therefore, past work proposed a manual adjustment of RSS signals to reduce positional error [14,15], which is not scalable as the number of new devices increases. In this respect, some works such as Tsui et al. [20] reduced the training time between devices to realize faster precalibration. Nevertheless, training for all brands of smartphones is still impractical because of the time and money cost. Therefore, free-calibration methods have drawn considerable attention recently. A typical free-calibration method uses similarity metrics at the online match phase instead of conventional distance metrics, i.e., Euclidean distance. The similarity metrics such as cosine/Pearson/Spearman similarity have been heavily addressed in past works [14,21–23]. However, the stability of this method remains a challenge because of its assumption that the RSS differences caused by hardware is constant; however, the differences are unknown. Moreover, this approach is mathematically less reliable if the dimensions of the calculated vectors are insufficient [8].

Another type of free-calibration method is the RSS difference method, and the basic rationale behind this method is the differential of the RSSs between APs or between positions, can minimize the effects created by heterogeneous devices. For example, as the user is walking towards an AP, he will obtain increasing RSS measurements with high probability, regardless of the AP's absolute transmission power and the model of the sensing device [8]; this is called the RSS gradient, which is basically a differential RSSs between positions. In contrast, the other RSS difference methods, including the SSD [13], DIFF [24] and MDF [25], leverage the RSS difference between APs. In particular, the SSD approach draws the most attention; Liu et al. [26] and Kjrgaard and Munk [27] developed a hyperbolic positioning algorithm based on the distance differences that are converted from SSDs and

minimized the positional errors. Unlike the geometric SSD approach, Hossain et al. [13] proposed a location fingerprint with SSD and demonstrated that it outperforms the traditional RSS fingerprint analytically and experimentally. Nevertheless, the SSD fingerprint amplifies the noise level and loses the discriminative information, leading to a potential reduction in accuracy compared to the raw RSS fingerprint with homogenous devices [28,29]. In this study, our PSSD system modifies the SSD fingerprint to make it more robust, and leverages the similarity metric to optimize the localization as well.

The RSS variation is another key factor towards accurate Wi-Fi positioning systems. However, the RSS observable is susceptible to the phenomena of interference, jumping, and instability, which are caused for many [8] such as the time-varying environments, human body blockage, and other unpredictable outliers. From the authors' point of view, there are two types of solutions to mitigate the large positional errors caused by RSS random variation. The first solution departs from the perspective of RSS variation and its cause. For instance, Wu et al. [16] uncovered outdated RSS in real-time measurements and developed a robust regression to tolerate this type of outlier. Fet et al. [30] suggested collecting orientation-dependent fingerprints for multiple directions to reduce the errors created by human blockage. Haeberlen [14] proposed a linear RSS transformation formula to compensate for environmental change, etc. However, these methods usually require considerable labor while offering minor improvement [16] and none of these methods has considered all aspects of the causes of RSS variation.

Another solution for mitigating the large error is the fusion with additional localization sources through Kalman filtering or particle filtering [31,32]. In a typical scenario of ubiquitous localization, the PDR is usually the primary option for fusing Wi-Fi because of its accurate positioning in a short time. Intensive experiments on PDR/Wi-Fi fusion have been conducted, and found a significant positioning precision improvement [33–35]. Despite the improvements, unstable human locomotion while walking and accumulated errors in inertial sensing make single-state PDR inapplicable for all states [36,37]. Therefore, fusion of Wi-Fi and single-state PDR in terms of the absolute walk heading/distance per step is not universal. Based on the previous work, our PSSD approach does not adopt the fusion scheme but directly increases the diversity of fingerprints to realize error mitigation, and in this sense, it is more similar to the first solution. Nevertheless, the diversity gain of fingerprints in PSSD comes from the spatial constraints offered by the range estimation of PDR's heading/distance within two Wi-Fi scans. Compared to the absolute heading/distance estimation, the range estimation of heading/distance is only raw information, but it becomes more reliable. In summary, the proposed PSSD exploits the reliable PDR information in terms of the fingerprinting level instead of the positioning level and this kind of method has never been addressed before to the best of our knowledge.

3. Method

The proposed PSSD approach enhances the usability of Wi-Fi positioning through leveraging three features: the SSD radio map, the spatial information extracted from PDR, and the pairwise RSS radio map.

In the offline training phase, a radio map called PSSD is constructed. The PSSD contains two layers: the first layer is based on the SSD approach to mitigate the hardware differences between smartphones, and the second layer is based on the pairwise RSS approach that exploits the geometric relation between reference points. Thus, we clarify the combination of these two radio maps in that (1) the SSD approach slightly lowers the location accuracy compared to the traditional RSS, thus SSD is only used to determine a series of candidate positioning points rather than the ultimate point, (2) the pairwise RSS approach is designed for minimizing large location errors at the price of a higher computational load than the normal method, and thus, selection of the best-fitting point from the candidates in previous step rather than the whole radio map can largely reduce the computational cost.

During the positioning inference phase, the RSS observables are first transformed into the SSD format to pick up five candidate match points from the prebuild SSD radio map. Subsequently,

the spatial information inferred by the step detection and heading estimation from PDR are extracted. In addition, the RSS measurements are transformed into a pairwise format, which is marked with the spatial information extracted in the previous step. Thus, the final best-fitting positioning point can be determined from the previous five candidates through the pairwise RSS radio map. The overall working flowchart of the proposed PSSD is shown in Figure 1. We will detail each module in the following subsections.

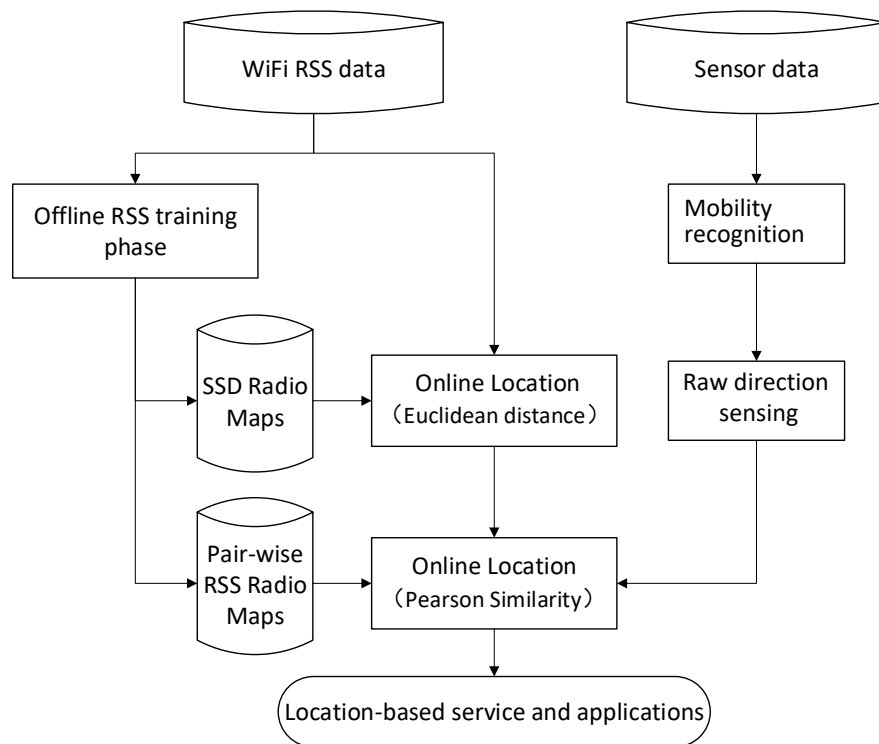


Figure 1. Overall working flowchart for proposed Pairwise Signal Strength Difference (PSSD) approach.

3.1. SSD Radio Map Construction and Online Inference

Generally, the samples' RSS values collected over a small time window are averaged to constitute the radio map in the offline phase for a deterministic KNN method [38]. However, having a different device in the online positioning phase would likely lead to a systematic bias of the RSS signature at the same location, and consequently lead to a mismatch with the already-built radio map. This can refer to the log-normal shadowing model for the traditional RF transmitter-receiver pair, as below [39]:

$$P(d)|_{dBm} - P(d_0)|_{dBm} = -10\beta \log\left(\frac{d}{d_0}\right) + X_{dB} \quad (1)$$

where $P(d)$ denotes the RSS at an arbitrary distance d from the transmitter, and d_0 denotes the reference distance such as 1 m. The β on the right side of Equation (1) denotes the mass loss exponents, while the second term X_{dB} reflects the signal variation that is subject to the Gaussian distribution ($X_{dB} \sim N(0, \sigma_{dB}^2)$). It should be noted that the perceived power $P(d_0)$ at the reference point depends on the device collecting the data, evidenced by the free space propagation model [40] as shown below,

$$P(d_0)|_{dBm} = 10 \log\left(\frac{P_{AP_i} G_{AP_i} G_{device} \lambda_{AP_i}^2}{16\pi^2 d_0^2 L}\right) \quad (2)$$

where P_{AP_i} is the i th AP's transmitted power, G_{AP_i} is the i th AP's antenna gain, G_{device} is the end-device's antenna gain, L is the system loss factor, and λ_{AP_i} is the transmitting carrier's wavelength. It is apparent that the term G_{device} makes the RSS measurement relevant to the device. Rather than using absolute RSS values as location fingerprints, we show that the difference in the RSS values observed by two APs (i.e., SSD) can be used to define a more robust signature for a transmitting mobile device; see a simple demo in Figure 2. With Equations (1) and (2), we directly present the mathematical form of SSD (denoted as δ) for the i th and j th APs without any deduction as follows:

$$\begin{aligned} \delta_{AP_i,j}|_{dB} &= P(d_i)|_{dBm}^{AP_i} - P(d_j)|_{dBm}^{AP_j} \\ &= 10 \log\left(\frac{P_{AP_i} G_{AP_i} \lambda_{AP_i}^2 L_j}{P_{AP_j} G_{AP_j} \lambda_{AP_j}^2 L_i}\right) - 10\beta_i \log\left(\frac{d_i}{d_0}\right) + 10\beta_j \log\left(\frac{d_j}{d_0}\right) + [X_i - X_j]_{dB}. \end{aligned} \tag{3}$$

More details about the formulation of Equation (3) can be found in Hossain et al. [13]. As we can see in Equation (3), SSD contains no device-relevant parameters (i.e., G_{device}) when compared to the absolute RSS shown in Equation (2), and consequently does not suffer from the device-different effect in theory. To support this, we conduct an experiment at three arbitrary training positions using three brands of mobile phones, see Figure 3.

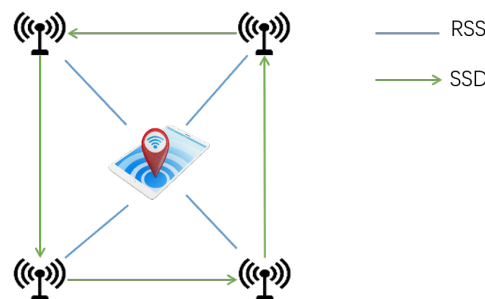


Figure 2. The usage of RSS and SSD from multiple APs.

The left panel of Figure 3 denotes the conventional RSSs measured by smartphones where it can be seen that the differences between the RSS curves can constantly reach up to 15 dB, which might be intolerant for RSS fingerprinting system. Instead, the SSD depicted by the right panel of Figure 3 has manifested a better consistency between mobile phones. Therefore, when not considering the noise level, the SSD fingerprint should be more desirable for heterogeneous devices. However, according to the error propagation law, SSD has a lower signal-to-noise level than RSS due to the term $[X_i - X_j]_{dB}$ that amplifies the noise variance to $\sqrt{2}\sigma_{dB}$. This side effect is unavoidable and slightly affects the localization accuracy that will be shown later in an experiment. Apart from this point, we also note that the freedom of SSD observations is less than that of RSS. For instance, at the i th round of the Wi-Fi scan, we obtain the RSS observations F_i as follows:

$$F_i = [S_1, S_2, \dots, S_n, \dots, S_{N-1}, S_N], \tag{4}$$

where S_n denotes the RSS of the n th AP. In addition, after converting the RSS to SSD by Equation (3), we find:

$$D_i = \begin{bmatrix} 0 & S_1 - S_2 & S_1 - S_3 & \dots & S_1 - S_n & \dots & S_1 - S_N \\ & 0 & S_2 - S_3 & \dots & S_2 - S_n & \dots & S_2 - S_N \\ & & 0 & \dots & \dots & \dots & \dots \\ & & & 0 & S_m - S_n & \dots & S_m - S_N \\ & & & & 0 & \dots & \dots \\ & & & & & 0 & S_{N-1} - S_N \\ & & & & & & 0 \end{bmatrix} \tag{5}$$

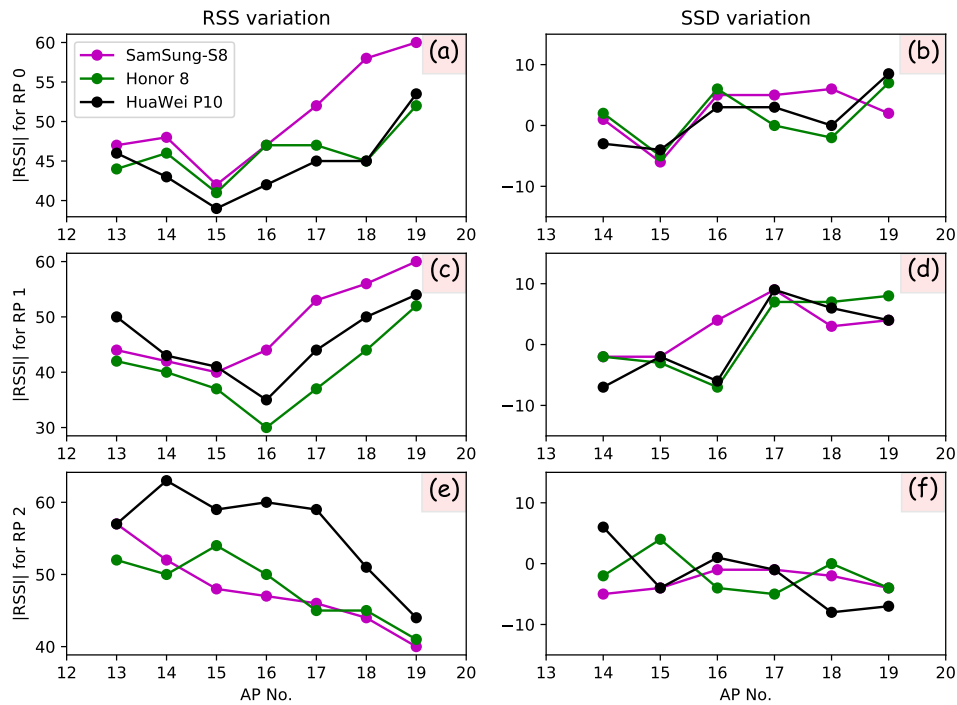


Figure 3. RSS versus SSD on three arbitrary reference points (RPs) collected by a Samsung-S8, Honor 8 and Huawei P10. (a,b) are performed on RP No. 0, (c,d) are performed on RP No. 1, and (e,f) are performed on RP No. 2.

A direct use of Equation (5) may lead to a high computational burden due to the high dimensions, so that a simplification of Equation (5) is necessary. It is apparent that the matrix form of SSD denoted by D_i is highly correlated, and the freedom of D_i is only $N - 1$ if we extract the maximal linearly independent group to present D_i as below:

$$D_i = [S_1 - S_2, S_2 - S_3, \dots, S_n - S_{n+1}, \dots, S_{N-2} - S_{N-1}, S_{N-1} - S_N], \tag{6}$$

Previous literature usually implemented the SSD algorithm according to Equation (6) without more consideration. Here, we note that many previous studies prefer to carry out experiments in an environment that researchers are familiar with. For instance, they normally distribute the APs at specified locations as uniformly as possible in advance and ensure that the APs are strong enough to cover almost all the experimental environment. However, this is inconsistent with reality, because you can never have knowledge of the precise location and the coverage of each AP at a shopping mall that you have never accessed before.

Therefore, a potential risk of Equation (6) would arise in practice when you have no predeployed APs. Assuming that the S_2 is not accessible for one round of Wi-Fi scan, SSD D_i will, therefore, lose two dimensions ($S_1 - S_2$ and $S_2 - S_3$) while the RSS vector F_i will only lose one dimension, as follows:

$$F_i = [S_1, \overset{\text{missing}}{\underbrace{S_2}}, \dots, S_n, \dots, S_{N-1}, S_N],$$

$$D_i = [\underbrace{S_1 - S_2, S_2 - S_3, \dots, S_n - S_{n+1}, \dots, S_{N-2} - S_{N-1}, S_{N-1} - S_N}_{\text{missing}}], \tag{7}$$

Assuming that the number of missing APs is L , then the valid dimensions of RSS and SSD are $N - L$ and $N - 2L$, respectively. In addition, the occurrence of missing APs occurs quite often in practical Wi-Fi scans. Here, we conduct a test and summarize the results in Figure 4, from which it can be seen that the Samsung captured 42 APs at least and 58 APs at most. However, Mix2 captures 28~45 APs. Not mentioning the heterogeneous devices, this experiment tells us that some APs would be frequently missing during a Wi-Fi scan even for the same device. Obviously, the traditional SSD shown by Equation (6) is not robust for this case, and thus, we attempt to modify Equation (5) to strengthen the stability of the SSD. Considering Equation (5), we extract another linearly independent group as complementary to Equation (6), and thus formulates the ultimate form of our SSD as shown below,

$$D_i = [S_1 - S_2, S_2 - S_3, \dots, S_n - S_{n+1}, \dots, S_{N-2} - S_{N-1}, S_{N-1} - S_N, S_1 - S_3, S_2 - S_4, \dots, S_{n-1} - S_{n+1}, \dots, S_{N-3} - S_{N-1}, S_{N-2} - S_N, S_{N-1} - S_1], \tag{8}$$

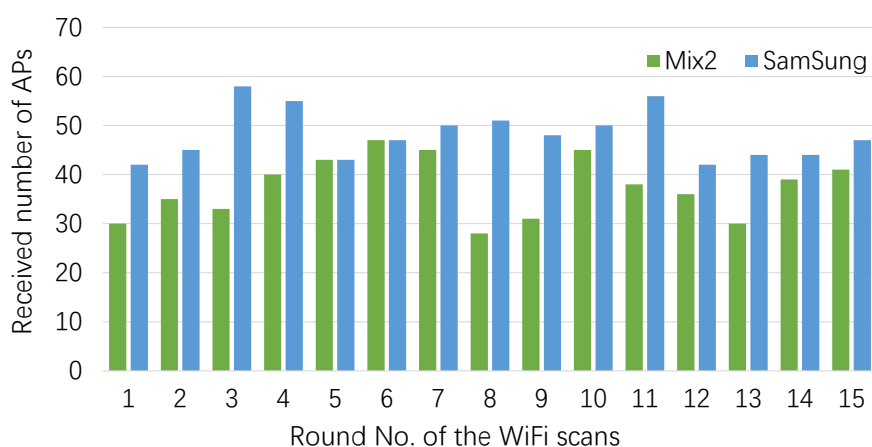


Figure 4. Number of APs detected for each round of Wi-Fi scans in terms of Mix2 and the Samsung S8. Here, 15 rounds of scans are summarized, and it is noted that Mix2 is a brand of smartphone produced by Xiaomi in China.

According to Equation (7), the dimensions of SSD increase to $2N - 3$. Thus, the missing AP_3 only causes the valid dimension (linearly independent) of SSD to decrease by 1 rather than 2. In addition, we believe that our SSD could better deal with the heterogeneous device problem than the previous SSD approach, and the only price is the additional computational load due to the increasing dimensions. Thus, for both the online and offline stages, the original RSS must be reformatted to the SSD as the pseudo-observations and the radio maps. Subsequently, the normal KNN with $K = 5$ and Euler distance metrics are applied to select the five best-fitted candidates from the dataset. However, unlike the previous works that tend to average the K candidates, we transfer these candidates to the next step to have a further selection, and therefore, a relatively large K such as $K = 5$ is empirically preferred. We note that the term “SSD” in the following denotes our modified SSD instead of the previous original SSD if there are no particular statements.

3.2. Spatial Mobility Information Extraction

The nature of the pairwise RSS approach is based on the fact that the user can only move within a limited distance between two Wi-Fi RSS scans. The pairwise RSS maps can be labeled with the spatial geometric information beforehand and further optimize the online inference procedure with the user’s mobility information. Before extracting the pedestrian’s mobility information, there are three questions that need to be answered. (1) How long is the time period between RSS scans? (2) How far can the pedestrian walk during the period? (3) What is the pedestrian’s heading during the period. These questions are key for constraining the search in the radio map. Figure 5 shows the possible range of a

pedestrian's walk distance/heading in different modes between Wi-Fi scans, and this raw information is coupled with the spatial topological relations between reference points.

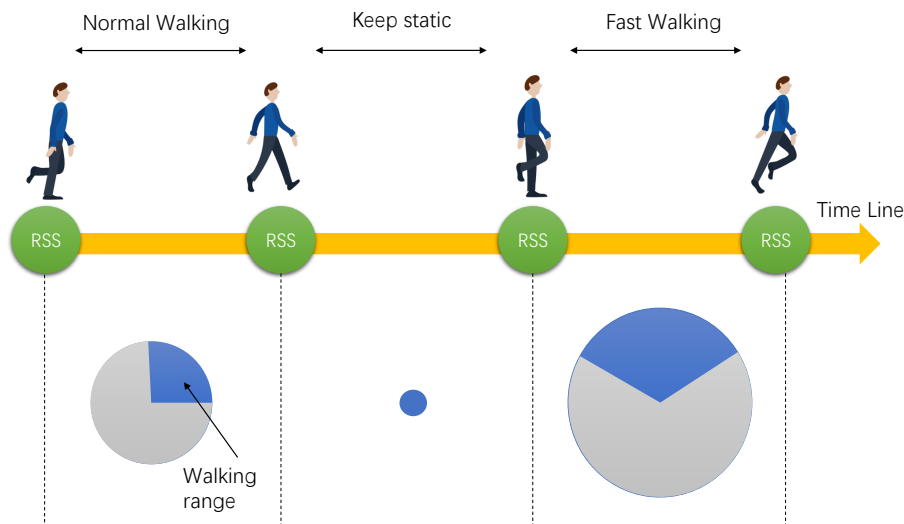


Figure 5. An example of a pedestrian's possible walking status while constantly receiving the Wi-Fi RSS scans. Here, the walking speeds are classified into fast, static and normal modes, and each of the speeds corresponds to a predefined walk range denoted as the gray solid circle. Meanwhile, the range of the pedestrian's walk direction between RSS scans is recorded and denoted as the blue sectors.

To answer the first question, we conduct an investigation of the average scan time between two valid RSSs (excluding invalid scans such as the repeated scans), on the most popular brands of smartphones (with Android platform only) in our daily life. We find that the valid RSS scan period for most smartphones is at [1.5, 2.5] seconds after 100 scans for each phone. Actually, most smartphones at normal working status require at least 1.2 s to finish one round of Wi-Fi scanning because an access point broadcasts a beacon approximately every 100 ms so that in theory, the device requires at least 1.2 s across the 12 frequency channels to scan all the access points.

To question two, step frequency in indoor environments ranges primarily from 1 Hz (slow walk) to 3 Hz (walking briskly or running) [41], and it is approximately 1.5 Hz in normal mode. To verify this, a step detection framework has been designed as follows. Due to the physiological characteristics of the pedestrian, the waveform of the accelerometer values (norm of the three-axis values) contains some particular cyclical characteristics and thus can be used to detect the step update. According to the characteristic, our system framework comprehensively includes three techniques. (1) A moving averaging window of length 15 to filter the high-frequency noise at the i_{th} accelerometer raw data Acc_i^{raw} , see Figure 6 left panel. (2) A peak detection to prevent small jitters by applying a threshold of peak value (Acc^{peak}) and interval (ΔT) between every two adjacent peaks, see Figure 6 right panel. (3) A zero-cross detection with adjacent accelerometer measures to find the step end, see Figure 6 right panel. In summary, a valid step should satisfy the following,

$$\begin{cases} Acc_i^{raw} = \sqrt{a_x^2 + a_y^2 + a_z^2} - g \\ Acc_i^{smooth} = (\sum_{j=i-14}^{j=i} Acc_j^{raw}) / 15 \\ Acc^{peak} > Acc_{Threshold} \\ \Delta T > \Delta T_{Threshold} \\ Acc_{i-1}^{smooth} > 0, Acc_i^{smooth} < 0 \end{cases} \quad (9)$$

where the a_x, a_y, a_z denote the three-axis accelerometer values and g denotes the local gravity acceleration. Herein the $Acc_{Threshold}$ is taken as 0.7 m/s^2 , and $\Delta T_{Threshold}$ is taken as 260 ms in our experiment given that the pedestrian is carrying the phone in “typing” mode. Another experiment is conducted to validate our step detection scheme, see Figure 7. The detected steps (in green circles) amount to 67, which is the same as the ground truth. In particular, a deeper insight into Figure 7 shows that the 67 steps occurred during 40 s, and this supports that the pedestrian’s step frequency is approximately 1.5 Hz. Assuming that the stride length is approximately $0.6\sim 0.8 \text{ m}$, then we can infer that the normal walking speed is approximately $1\sim 1.2 \text{ m/s}$, and thus, the pedestrian can walk a distance of 3 m between two RSS scans in the period of $[1.5, 2.5] \text{ s}$. Similarly, the pedestrian in a fast mode will walk a distance of 6 m between two RSS scans. The recognition of normal mode and fast mode can be realized by the step detection strategy or machine learning, yet the discussion is obviously beyond the scope of this paper.

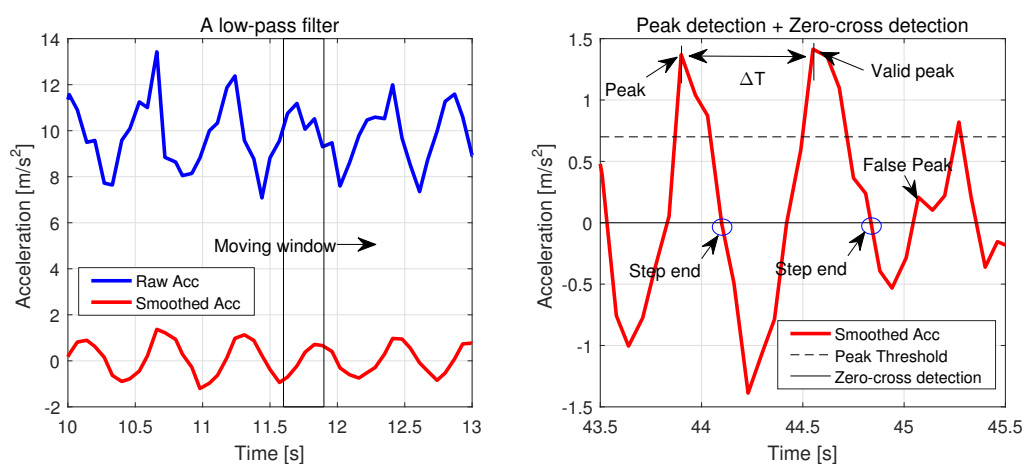


Figure 6. The left panel denotes the low-pass filtering method by a moving averaging window, and the right panel shows the peak selection and the determination of step end. The occurrence of a valid peak and step end within one cycle will account for one step.

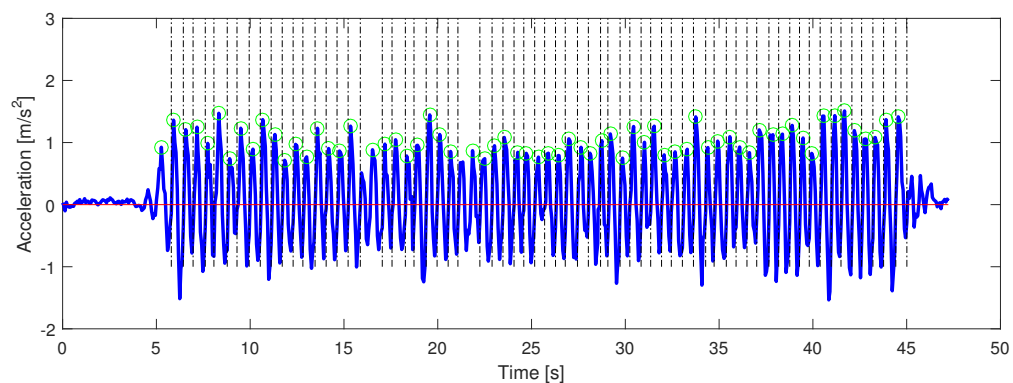


Figure 7. An experiment of a pedestrian walking at the normal status (ground truth is 67, and the detected step count is also 67). The green circle represents the detected steps, and the subsequent black dashed line denotes the finish time of this step.

Let us consider question three; that is, what is the pedestrian’s heading range during the period? First, we know the yaw of the pedestrian can be estimated from the acceleration sensor, magnetic sensor, and gyroscope sensor. The fusion of these sensors is performed through the quaternions complementary filter. Quaternions offer an angle-axis solution to rotations which do not suffer from many of the singularities, including gimbal lock, that are found with rotation matrices.

A complementary filter is used to fuse the two orientation estimations (the gyroscope θ_{gyro} and acceleration/magnetic $\theta_{acc/mag}$) together in the frequency domain, as below,

$$\theta_{fusion} = \alpha \int \dot{\theta}_{gyro} dt + (1 - \alpha)\theta_{acc/mag}, \quad (10)$$

In above equation, α is defined as $\alpha = timeConstant / (timeConstant + dt)$, where the *timeConstant* is the length of the signals the filter should act on, and *dt* is the sample period (1/frequency) of the sensor. The implementation of this algorithm is performed by publicly available software, namely, Fsensor provided by <https://github.com/KalebKE/FSensor>. A static test on this algorithm shows the standard deviation is within 3 degrees. However, considering the environmental disturbance from both the pedestrian and magnetic abnormality, we empirically set the uncertainty (3 times of the standard deviation) to 10 degrees. Thus, a series of heading angles $A_{t_{i-1}}^{t_i}$ can be acquired between any two moments (t_i, t_{i-1}), and furthermore, the range $R_{t_{i-1}}^{t_i}$ of the pedestrian's walk between two Wi-Fi scans can be derived by

$$\begin{aligned} A_{t_{i-1}}^{t_i} &= \bigcup \theta_{fusion} \\ R_{t_{i-1}}^{t_i} &= [\min(A_{t_{i-1}}^{t_i}) - 10, \max(A_{t_{i-1}}^{t_i}) + 10] \end{aligned} \quad (11)$$

In summary, in static mode, the user's walk range is less than a minor quantity such as 0.1 m, see Figure 5; in fast/normal mode, the range changes to 6 m and 3 m, respectively, manifested as the radius of the circles in Figure 5. Moreover, the heading range is also restricted within the blue sectors in Figure 5. This information constructs the spatial constraint that will be used later.

3.3. Pairwise RSS Radio Map Construction and Online Inference

Unlike the traditional radio map that uses the form of point distribution, the pairwise RSS map creates a vector-based format leveraging the spatial geometric information between reference points. Traditional RSS map construction is based on the RSS collection that requires the user to remain stationary, but this type of radio map is obviously inconsistent with the reality. The user's location is indeed moving but not fixed at the discrete points/nodes, and the RSS is also collected along the walking route but is not fixed at a certain time epoch. Thus, our work relates each node's RSS with its neighborhood, and in this way, reshapes the point-based RSS to a pairwise RSS.

Assuming that δ denotes the Euclidean distance between two nodes, then the set of neighborhoods of a given node a in the radius δ^* can be derived as

$$U(a, \delta^*) = \{x \mid |a - x| < \delta^*\}. \quad (12)$$

where the δ^* is optional, such as 3 or 6 m. The traditional fingerprint at node a is denoted F_a (see, Equation (4)), and we thus define the pairwise fingerprint $P_{a,b}$ for the center node a and its neighbor node b as below,

$$P_{a,b} = [F_a, F_b] = [S_1^a, S_2^a, \dots, S_n^a, \dots, S_{N-1}^a, S_N^a, S_1^b, S_2^b, \dots, S_n^b, \dots, S_{N-1}^b, S_N^b], \forall b \in U(a, \delta^*) \quad (13)$$

In addition to the added distance information, the new "vector" form of fingerprint can record the direction information as well. Given the coordinates of node a and b in the plane rectangular coordinate system, we derive the azimuth of a with respect to b as $\theta = \arccos(\frac{\vec{a} \cdot \vec{b}}{|\vec{a}| \times |\vec{b}|})$, which is appended to $P_{a,b} \mid_{\theta}$ as a label. If the traditional point-distributed RSS radio map has m reference points, as node a moves until the whole map is covered, a completely new fingerprint database, whose number of "reference points" should be subject to $\bigcup_{a=1}^m U(a, \delta^*)$ is created. It should be noted that the reference point in terms of its original form denotes the a or b that is actually a true point in the physical world, but herein the "reference point" induced from Equation (13) is simply a mathematical conception (a pair form of true points (a, b)) and has no physical content. Consequently, the best-fitting positioning point selected

from our radio map is the form (a, b) rather than a or b . However, there is a convention or mapping ζ defined by us between the vector result and the physical location; that is

$$\zeta : (x, b) \longrightarrow b, \forall x \in U(b, \delta^*) \tag{14}$$

where x denotes an arbitrary point distributed within the neighbor of point b , which means the pedestrian’s position referred by (x, b) is indeed the position of point b .

Apparently, the dimension or the number of “reference points” derived from $\cup_{a=1}^{a=m} U(a, \delta^*)$ has greatly exceeded the original number m of the true reference points, and it continues to increase as δ^* increases. Within expectation, the computational load of online inference in terms of this very large database (too large δ^*) will be intolerant. To prevent the very large database problem that may lead to the infeasibility of KNN, we decrease the neighborhood range according to our experience from the previous subsection, which means δ^* is only set to 3 m and 6 m (see Figure 8). Moreover, we restrict the number of candidate reference points ($m = 5$) offered by the SSD approach, and by combining with the heading information, the dimensions of the real-time fingerprint database are significantly reduced, which will be demonstrated later.

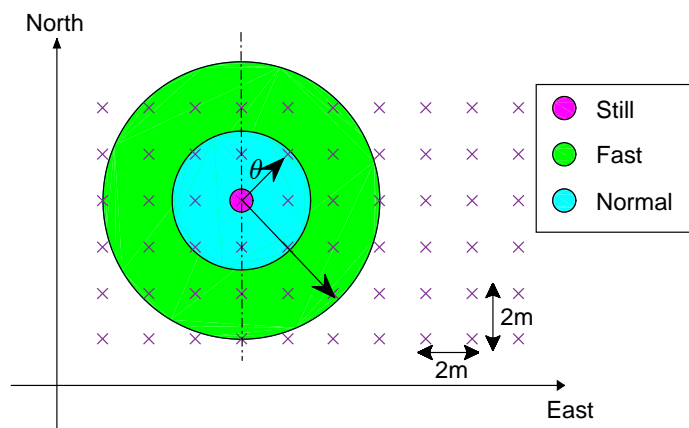


Figure 8. An example of the construction of a pairwise RSS fingerprint database associated with the topological information. Three types of topological information are demonstrated for the still, fast, and normal modes. Please note that we set the grid length to an average of 2 m in accordance with the general performance of fingerprinting-based positioning methods.

In the online phase, the current i_{th} RSS measurements F_i must be transformed as well to remain in accordance with the pairwise RSS fingerprint database. Hence, the current RSS and the previous RSS are combined into a new measurement $M_{i-1,i}$ as shown below:

$$M_{i-1,i} = [F_{i-1}, F_i] = [S_1^{i-1}, S_2^{i-1}, \dots, S_n^{i-1}, \dots, S_{N-1}^{i-1}, S_N^{i-1}, S_1^i, S_2^i, \dots, S_n^i, \dots, S_{N-1}^i, S_N^i], \tag{15}$$

In addition, the current walking status between two RSS scans, recognized by the step detection algorithm or machine learning, is recorded as well, including three major modes: still, fast, and normal. The classified three modes correspond to three different fingerprint databases $\cup_{a=1}^{a=m} U(a, \delta^*)$. In more details, $\delta^* = 0.1$ for the “still” mode, $\delta^* = 3$ for the “normal” mode, and $\delta^* = 6$ for the “fast” mode. Simultaneously, the heading range $R_{t_{i-1}}^i$ of the pedestrian is recorded as well, according to Equation (11). The walking speed and heading range are the pedestrian’s mobility information that will determine the pedestrian’s relative positions between RSS scans.

Subsequently, unlike the previous work that establishes a radio map and keeps it constant in online inference phase to locate the optimal position point, our radio map or the fingerprint database is only one subset of the whole database and it adaptively changes continuously according to the

varying spatial information induced by the pedestrian’s mobility. Every time the RSS (F_i) is updated, we retrieve a subset of the radio map (named after Pmap, and $Pmap \subseteq \bigcup_{a=1}^{a=m} U(a, \delta^*)$) as shown below:

$$Pmap_i = \{P(a, b) | \theta \in R_{t_{i-1}}^i, \delta^* \in \{0.1, 3, 6\}, b \in C\} \tag{16}$$

where C is the union of five candidate positioning points from the SSD approach, and θ is the angle information for vector (a, b) that was previously derived. Thus, there is a one-to-one corresponding (measurement $M_{i-1,i}$, database $Pmap_i$) map that is built simultaneously. In addition, the online match algorithm adopts the KNN with the distance metric of Pearson similarity. Considering two groups of measurements such as $A = (A_1, A_2, \dots, A_n)$ and $B = (B_1, B_2, \dots, B_n)$, the similarity between these two vectors in terms of the Pearson coefficient is,

$$S(A, B) = \frac{\sum_1^n ((A_i - \bar{A}) \times (B_i - \bar{B}))}{\sqrt{\sum_1^n (A_i - \bar{A})^2} \times \sqrt{\sum_1^n (B_i - \bar{B})^2}} \tag{17}$$

Use of similarity as the distance metric within the KNN algorithm has the advantage on minimizing device differences, which was discussed in the introduction. In addition, the dimension increase of $P_{a,b}$ with respect to F_b makes the similarity metric more reliable. Finally, we summarize the online match procedures (shown by Equation (18) as well as Figure 9) that (1) the RSS map in terms of reference points are transformed into pairwise fingerprints beforehand, (2) in the online inference phase, the previous RSS measurement and the current measurement are grouped and reformatted to the pairwise form, (3) subsequently the spatial information including the walking speed and heading range are derived to select a subset $Pmap$ from the whole fingerprint database, and (4) finally, the new pairwise measurement is compared to $Pmap$ and to locate the user’s position with the Pearson similarity metric. Please find all the procedures in Figure 9.

$$\arg \max_x (S(M_{i-1,i}, x), \forall x \in Pmap_i) \implies x_{S_{max}} \implies (a, b) \implies b \tag{18}$$

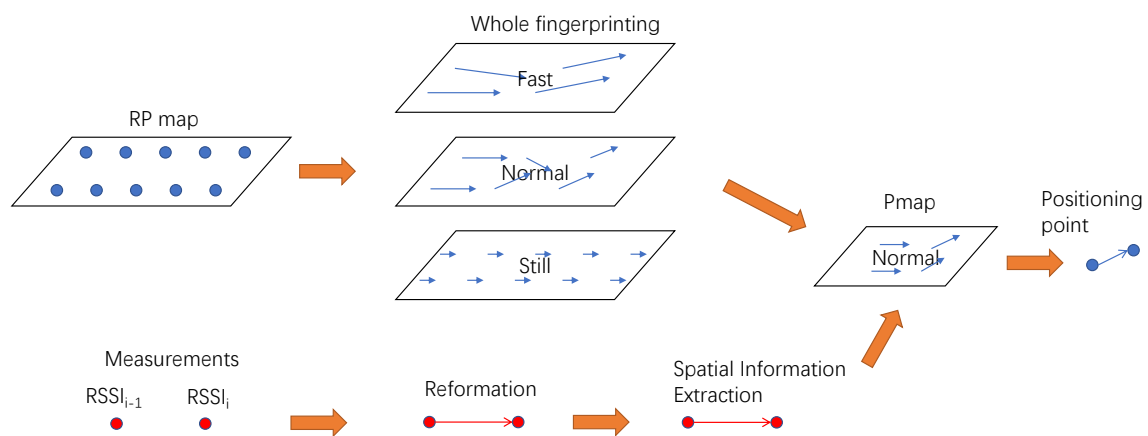


Figure 9. The generation of the Pmap in terms of “vector” form from the classical RSS radio map in terms of the reference point (RP), and the online inference procedure with the Pmap and the reformatted measurements leveraging real-time mobility information.

4. Experiments and Results

In this positioning experiment, the mean error, root-mean-square (RMS) error, and the 95% error in the positioning results of the three fingerprinting algorithms are compared in different actual scenarios. The objective of the experiments is to compare the positioning performance of the proposed PSSD algorithm with that of two legacy algorithms, SSD and RSS fingerprints. It should be noted that

all these fingerprinting algorithms are based on the deterministic method (KNN) to locate the final positioning point.

4.1. Static Test for SSD Method

As mentioned in previous, the traditional SSD theoretically suffers from dimension loss because of missing APs, see Equation (6). In this context, we propose a modification of SSD (namely, MSSD) to mitigate the dimension loss effect, see Equation (8). Here, we conduct a test at a static environment to compare these two methods. An empty hall of our laboratory was selected as the test field, where 20 reference points (numbered from 0 to 19) are distributed uniformly on the floor with an interval of about 2 m (horizontal 2.2 m and vertical 1.8 m), see Figure 10a. The Samsung S8 was chosen to establish the fingerprints. In the offline training phase, we collect the RSS information at each reference point for 30 rounds, and finally average the 30 times of scans to establish the traditional RSS fingerprint according to Equation (4). In the online phase, the user was asked for standing still at each reference point to collect 15 rounds of RSS with Samsung S8 and XiaoMi, respectively. Therefore, the ground truth is easily recorded and 300 groups of measurements for each smartphone in total are evaluated to compare the SSD and MSSD approaches. It should be noted that to isolate the errors caused by varying environments and the body blockage, the user was asked for keeping the same gesture and direction at online and offline phases, moreover the online measurements were collected soon after offline training.

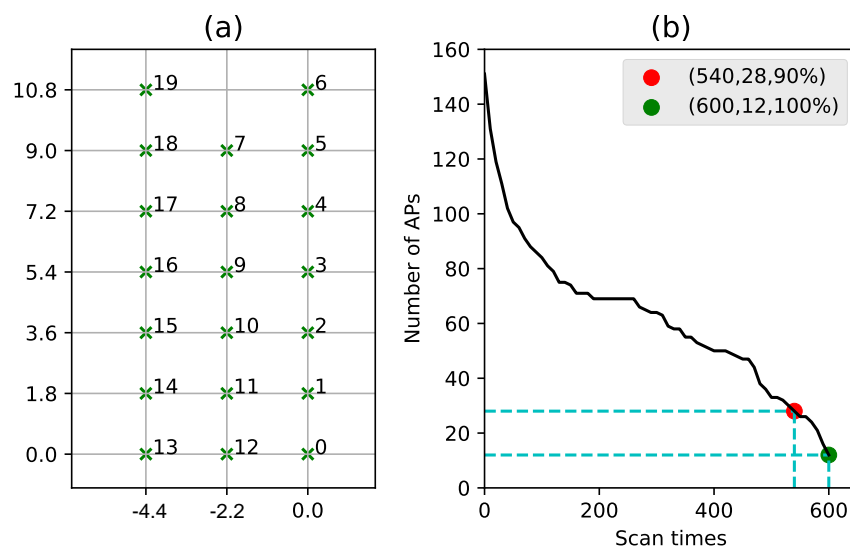


Figure 10. (a) The floor map and the reference points' spatial distribution of the static test. (b) A total of 154 APs has been found at the training phase, but it does not mean the 154 APs can be detected for each scan. The Y-axis of (b) denotes how many APs can be detected over given times of scans (X-axis).

It is worth mentioning that not all APs that have been scanned can participate in the computation of KNN distance metrics. Prior to the fingerprint establishment, a proper selection of APs with good quality is crucial for online positioning performance. According to Equation (4), the AP selection is actually the procedure of dimension determination. Once the APs (dimension) are selected, the online measurements must be filtered to keep only the information from predefined APs, in accordance with the fingerprints. However, the online measurements of heterogeneous smartphones usually suffer from the missing AP problem (receiving no RSS values from the predefined APs) as mentioned before, which will undermine the positioning performance of no matter RSS, SSD, or MSSD methods. To mitigate the missing AP problem, the APs selected for establishing fingerprints should be as strong as possible, so that even the heterogeneous devices can detect it at most of the time.

In our experiment, a total of 154 APs during the 600 times of scans in the offline training phase were successfully found after removing the invalid ones, i.e., the personal Hotspot, see Figure 10b.

However, only 12 APs are found to be the common ones for the 600 times of scans (100%, see the green dot at Figure 10b), and it means that the 12 APs have relatively strong and stable signals. In addition, 28 APs are found to be scanned over 540 times (90% of the 600 scans, see the red dot at Figure 10b). To increase the dimension, we select these 28 APs rather than previous 12 APs to constitute the final fingerprints. In theory, the homogenous device has a high probability (90%) to detect the 28 APs at any place of the room in the online phase, while this probability does not suit for heterogenous devices.

Test results for homogenous smartphone (Samsung S8) and heterogenous smartphone (XiaoMi) are summarized at Table 1. As the ground truth of user's positions are just the positions of reference points, we introduce the successfully matched ratio (matching rate) as an important index to evaluate the positioning performance. It can be seen that in case of homogenous device (Samsung S8), the conventional RSS method reaches the highest matching rate (83.4%), and the least mean positioning error (0.48 m) as well as the RMSE (1.65 m). The advantage of RSS over SSD and MSSD in terms of homogenous device from Table 1 is consistent with the facts that (1) RSS has always at least one more dimension than SSD and MSSD, see Equations (4), (6) and (8); (2) the (M)SSD has a lower signal-to-noise level than RSS method as mentioned before. It is also worth mentioning that SSD and MSSD perform equivalently because they are basically the same if there are no missing APs (see Equations (6) and (8)). To validate this, we investigate the 300 online measurements of Samsung S8 and find that the 28 APs selected for constructing fingerprints are all detected every time, so there is no missing APs taking place at all.

Table 1. Static test results for Samsung S8 and XiaoMi smartphones. It is noted that each phone collected 300 online measurements, and Samsung S8 collected the fingerprints. The unit of mean positioning error as well as RMSE is [m].

Smartphone	Test Approach	Matching Rate	Mean Error	RMSE
Samsung S8	RSS	83.4%	0.48	1.65
Samsung S8	SSD	82.0%	0.85	1.96
Samsung S8	MSSD	82.0%	0.85	1.96
XiaoMi	RSS	6.7%	3.79	4.60
XiaoMi	SSD	18.7%	2.86	3.53
XiaoMi	MSSD	22.1%	2.64	3.28

In case of heterogenous devices (XiaoMi), it can be found from Table 1 that the matching rate declines significantly for all approaches (i.e., RSS approach: from 83.4% to 6.7%), which means the zero-error positioning is far less than that of Samsung S8. Meanwhile, the mean error and RMSE of XiaoMi increase dramatically, for instance, the mean error of RSS approach gains from 0.48 m to 3.79 m. In particular, the conventional RSS approach has severely deteriorated compared to the homogenous device, showing that the device difference is one of key factors that undermine fingerprinting-based positioning performance. However, the SSD as well as MSSD approach attributed to its differential format has somehow reduced the influence of device difference and enhanced the positioning performance (the mean errors of SSD and MSSD are 2.86 m and 2.64 m), compared to the RSS approach (the mean error is 3.79 m).

In addition, unlike the previous case of homogenous device (Samsung S8 achieves an equivalent performance for SSD and MSSD), the MSSD slightly outperforms than SSD in terms of XiaoMi. To reveal the reason, we investigated the 300 online measurements of Xiao Mi and found that the 28 APs selected for constructing fingerprints are all detected for only 110 times, and for the rest times there are always several (1~8) missing APs taking place. As MSSD approach can better handle with the dimension loss problem caused by missing APs, its positioning performance has a slight enhancement compared to conventional SSD approach (mean error 2.86 m versus 2.64 m). Despite of a limited improvement, we suggest that the proposed MSSD is effective.

4.2. Testbed Setup for PSSD Method

We implemented the Wi-Fi fingerprinting-based positioning on an Android platform, including the RSS, SSD, and our PSSD methods. It is noted that the SSD in the following indeed denotes the MSSD in previous subsection. An in-house application HIPE was developed for not only simultaneous indoor positioning (see Figure 11 upper panel) but also for collecting Wi-Fi fingerprints along the reference points in the offline phase (see Figure 11, the red dots on the bottom panel). Our indoor floor plan is visualized by a commercial toolbox called Mapbox, which can be found at <https://www.mapbox.com/>. In particular, we construct the indoor map in terms of the WGS-84 geodetic reference system [42] to remain consistent with the outdoor map offered by Mapbox. In the positioning mode, our HIPE application runs the Wi-Fi thread and PDR thread at the same time. The sampling rate of the IMU sensor data is set to approximately 50 Hz (the “GAME” mode according to the Android API), and the Wi-Fi scans continuously approximately every 2 s. In the radio map construction mode, the HIPE application collects the Wi-Fi scan results at given reference points and simultaneously records the corresponding coordinates through the Mapbox API, as shown in Figure 11. Additionally, we set landmarks at each reference point, so that the ground truth positions of the user can be obtained when the users record the timestamp and the number of landmarks they pass. In addition, a linear interpolation of the landmarks’ positions is carried out to derive the pedestrian’s true position every time when RSS updates.

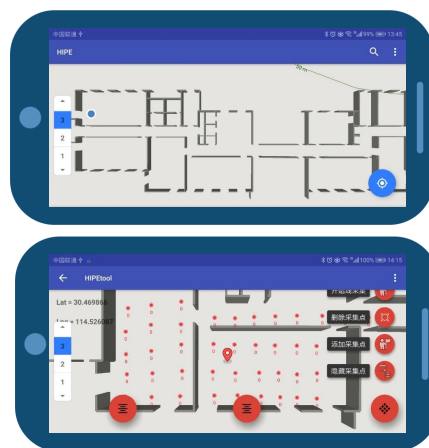


Figure 11. Screenshots of HIPE application: the top panel denotes the online localization, and the bottom panel denotes the construction of radio map.

We evaluate the HIPE application in a five-story office building, namely, Center of ShiLinTong, which is owned by Wuhan University. The experiments were carried out in public areas on the third floor with 75 m by 22 m in size, see Figure 12. The third floor is mainly composed of multiple meeting rooms, teacher offices, student computer labs, lobbies and a long straight corridor (marked in white in Figure 12). With this complex building structure, our experimental area includes most actual scenarios in daily life, making it similar to the reality. In addition, as the building is in normal condition for use, people are working routinely in their rooms and some occasionally walks around and passes by our user when collecting fingerprint database in the offline phase. The situation in the online phase is similar, so that the consistency of RSS measurements can be ensured. We note that the experiments (like those in many previous literature) are carried out under some relatively ideal assumptions. For instance, the surrounding people should be not too crowded, and the predefined paths for experiments are selected to be as uniform as possible (see Figure 12). Otherwise, very crowded environments will fail most of the state-to-art indoor positioning techniques including Wi-Fi fingerprinting, as far as we know.

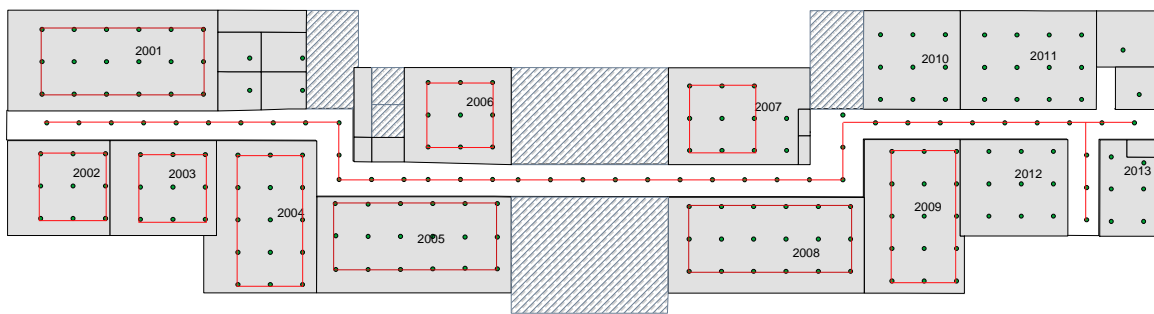


Figure 12. Our Wi-Fi fingerprinting experimental testbed—all the training locations (reference points) are marked as dark green points, and the office rooms are marked as the gray area. It is noted that the areas in shadow are unavailable locations. The red curves denote the predefined paths (starting from room 2005), which are designed along the reference points to ease the experiments.

We use two fingerprint-based localization approaches, the conventional RSS and the SSD mentioned before, as benchmarks in our experiments. Based upon our experience, it is impractical to dedicate vast amounts of computational and human resources to acquire data at each reference point to construct the radio map for each approach. However, SSD and the proposed PSSD can be transformed from an RSS-based radio map. In this context, we only need to collect data as required by the RSS radio map in the offline training phase. Therefore, 219 reference points were established on a grid map at intervals of approximately 2 m in public areas, such as the rooms and corridors, denoted as the dark green dots in Figure 12. To establish a reliable conventional RSS fingerprint database, 30 sets of sample data were first collected at each reference point by an Honor 8 smartphone, and subsequently, the mean value of each AP RSSI at a given reference point constituted the RSS fingerprints. It should be noted that the mean value was derived after removing the outliers with $3 - \sigma$ criteria. With the RSS fingerprints, the SSD fingerprints can be easily established according to Equation (8).

As for the pairwise RSS fingerprint, we note that it is not directly derived from Equation (13), because the pairwise fingerprint assumes the two points are connected (see Figure 8) while the walls in our test environment divided the whole space into several separate subspaces such as the offices and the corridor (see Figure 12). For example, a pairwise format between a point inside the office and a point inside the corridor will lead to the cross-wall error. To this end, the pairwise RSS is first constructed inside each subspace, which was numbered from 2001 to 2013 (see Figure 12), in addition to the corridor. Subsequently, the pairwise RSS fingerprints built from each subspace were accumulated as a whole, and this was the ultimate fingerprint database for later localization.

4.3. Overall Performance Evaluation

We first conducted experiments to verify our step count detection strategy, and during the experiment, the pedestrian was asked to walk at a normal pace and fast pace. The analysis of the step count error is shown in Table 1, and it should be noted that the true number of steps for each test group was always 100. As can be seen from Table 2, the overall performance of our step count strategy can ensure an accurate determination of the user's walking speed (normal/fast) with the additional timestamp information.

Table 2. Tests of step count detection.

Number of Tests	Walk Speed	Calculated Steps	Steps Error	Error Rate
1	Normal	98	2	2%
2	Normal	97	3	3%
3	Normal	97	3	3%
4	Fast	99	1	1%
5	Fast	100	0	0%
6	Fast	99	1	1%

Subsequently, another series of experiments were conducted to examine the robustness of PSSD among heterogeneous smartphones as well as its possible superiority with respect to RSS/SSD fingerprinting methods. Thus, the user was asked to hold the Samsung S8, Honor 8, and Huawei P10 smartphones free from constraints on the walking speed. In addition, the user kept walking for about ten minutes each time along the predefined paths that covered the test areas so that the ground truth of pedestrians' positions could be easily recorded. In addition, walking was repeated five times at different times of the day to ensure that enough samples were collected to run the performance evaluation. During the walk, all the Wi-Fi RSS scan results along with inertial sensor data were recorded as inputs for the three algorithms. The cumulative distribution function (cdf) of localization error is shown in Figure 13.

Figure 13a shows the test results of homogenous devices, where it can be found that the RSS method achieves an average accuracy of 2.5 m (see Table 3) that might be not good enough. We clarify that the causes of positioning errors may come from many sources, such as body blockage, environmental change, device differences, and the other unknown factors. These error sources are mostly varying and unpredictable, leading to a quasi-random error distribution without significant patterns, in particular at a large building where no prior information of APs is known (this is our case as well). In this sense, the positioning error (2.5 m) of RSS approach is reasonable, as it has no particular treatment with any of the error sources. With one step further, the SSD has specifically dealt with device difference problem, while the rest error sources remain. In contrast, rather than dealing with each error source directly, the proposed PSSD approach bypasses them and imposes the additional spatial constrain (user's mobility as prior information) to the fingerprinting procedure, so that the final positioning error can be reduced indirectly.

Unfortunately, the PSSD approach, which is developed from SSD, has completely inherited the SSD's ability to minimize device difference as well as SSD's side effect on homogenous devices discussed in previous subsection. Within expectation, a worse positioning performance of SSD and PSSD than RSS approach in terms of homogenous devices can be found at Figure 13a and Table 2 (see the mean error). Figure 13a has shown that the RSS curve lies higher than the SSD curve at the beginning, but eventually converges at the end, indicating that SSD performs slightly worse than RSS and large errors still exist. In addition, the PSSD curve approximately overlaps the SSD curve, but PSSD has slightly reduced the large errors regarding the SSD performance, as shown by the end of their curves. The depicted results are also consistent with our previous inference that RSS should perform best in terms of homogenous devices, but even in this case the PSSD has taken effect and mitigated some large errors, as shown by the maximal error and 90 percentile error in Table 2.

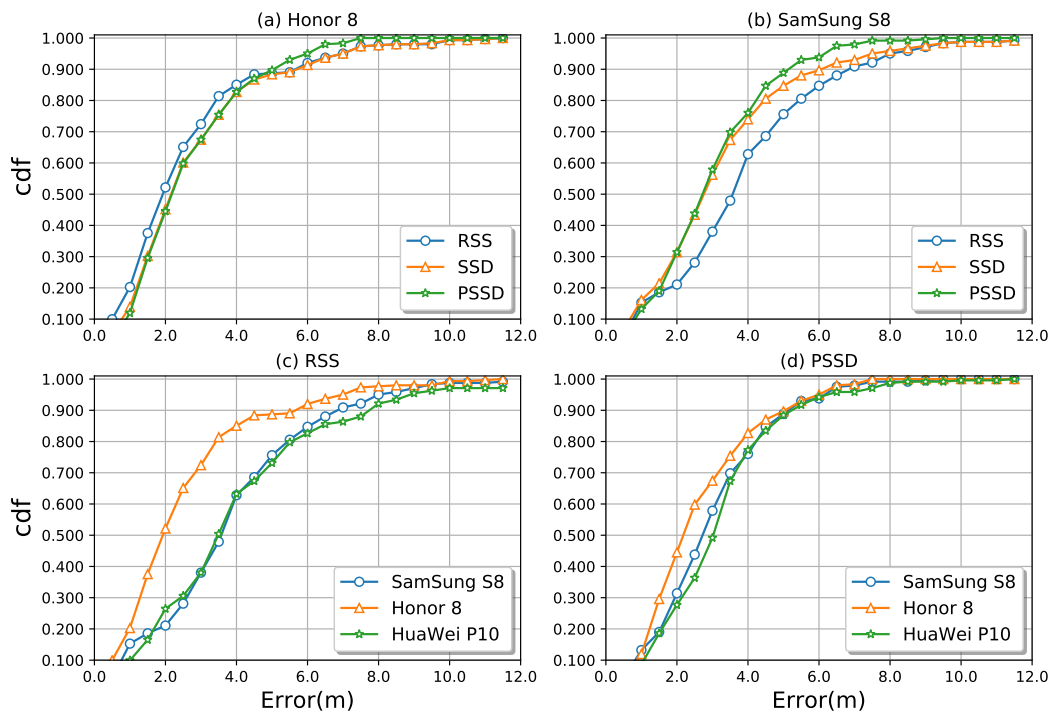


Figure 13. Localization performance in terms of fingerprints collected by Honor 8. (a) Comparisons of three approaches using the Honor 8 in online phase. (b) Comparisons of three approaches using the Samsung S8 at online phase. (c) Performance of the RSS approach using different devices. (d) Performance of the PSSD approach using different devices.

Table 3. Statistics of localization performance. The unit is [m].

Smartphone	Test Approach	Mean Error	RMSE	Maximal Error	90 Percentile
Honor 8	RSS	2.5	3.2	11.3	5.7
Honor 8	SSD	2.7	3.4	11.3	5.8
Honor 8	PSSD	2.6	3.0	7.1	5.1
Samsung S8	RSS	3.8	4.6	19.1	6.7
Samsung S8	SSD	3.2	4.0	19.1	6.0
Samsung S8	PSSD	2.9	3.3	9.1	5.2
Huawei P10	RSS	4.0	4.9	18.0	7.7
Huawei P10	SSD	3.2	4.2	19.2	7.0
Huawei P10	PSSD	3.1	3.6	11.1	5.3

In contrast, another insight into Figure 13b shows that the PSSD in terms of heterogeneous devices significantly enhances the localization accuracy with respect to the RSS approaches, for example, the mean errors derived from RSS and PSSD are 3.8 m and 2.9 m, respectively. Although the PSSD with the Samsung S8 could not reach the accuracy of RSS with the Honor 8 (i.e., the mean error was 2.5 m), we suggest that PSSD has well handled with the problem of device differences. Additionally, compared to SSD (the yellow curve in Figure 13b), the large errors decreased as expected, see also the maximal errors highlighted in Table 2. We realize that the improvement of PSSD over SSD mainly comes from the additional spatial constrain shown by Figure 8; however, the error sources such as body-blocking and temporal environmental change, which PSSD does not consider as well, still exist and undermine the positioning performance for both PSSD and SSD approaches.

Figure 13c,d separately demonstrated the performance of RSS and PSSD among different devices, from which we can see that the device difference is a dominant factor that affects the final localization accuracy as the Honor 8 largely outperformed the Samsung S8 and the Huawei P10 (see Figure 13c). Though our PSSD can mitigate the device differences to some extent, the Honor 8 still performed better than other devices. Therefore, we realize from the experiments that the impact from device differences is unavoidable and will be very challenging for our future work that aims to enhance the fingerprint-based localization accuracy. Finally, we conclude from Table 2 that the proposed PSSD approach in terms of heterogeneous devices has an overall improvement of approximately 20% compared to the conventional RSS approach, i.e., the mean error (3.8 m vs. 2.9 m, Samsung S8; 4.0 m vs. 3.1 m, Huawei P10), the RMSE as well as the 90-percentile error.

Above results demonstrate the overall positioning performance of three approaches; however, during the experiment we also realize the significance of the walking speed, which may considerably affect the performance, see Figure 9. To this end, an additional experiment specified on the speed influence was carried out by testing a heterogenous device (Samsung S8) in normal (<1.5 m/s) and fast walking mode (>1.5 m/s), respectively. Unlike the walk paths in previous, the predefined walk path this time is selected as a round-trip one along only the corridor, which lays from the left side to the right side of the floor map, see Figure 12 the area marked in white. The probability density distribution of positioning error is recorded in Figure 14.

Figure 14a compares the positioning performance of RSS approach in fast and normal modes. As the experiment employed a heterogenous device, RSS approach returns an unsatisfactory result, for instance, the mean errors in terms of normal mode and fast mode are 3.7 m and 4.3 m, meanwhile the 90-percentile errors are 5.9 m and 7.6 m, respectively. In general, the online RSS measurements are collected dynamically along the path; however, the offline fingerprints are collected by standing still. Therefore, a faster walking speed would induce a larger discrepancy between online RSS measurements and offline fingerprints, resulting in a larger positioning error. We thus suppose the discrepancy is one cause of the increasing error of RSS approach in fast mode. It is also worth mentioning that this discrepancy exists in the SSD and PSSD approach as well. By further investigating the Figure 14b,c), which compare the speed influence on SSD and PSSD approaches, we find a similar result as that found before in Figure 14a: the mean errors (2.7 m, SSD; 2.2 m, PSSD) in normal mode has increased to (3.3 m, SSD; 3.1 m, PSSD) in fast mode; the 90-percentile errors (5.5 m, SSD; 5.0 m, PSSD) in normal mode has increased to (6.4 m, SSD; 5.8 m, PSSD) in fast mode as well. It is apparent that the fast walking mode considerably lowers the positioning accuracy of no matter RSS, SSD, or PSSD approaches.

Another comparison could be made between RSS, SSD, and PSSD approaches. According to Figure 14 and its statistical mentioned above, we find that RSS behaves the worst and PSSD behaves the best in both speed modes, which is consistent with the results in previous experiments. However, the walking speed may have different influence on different approaches (excluding the discussion of RSS approach because the heterogenous device is used in this experiment). For instance, Figure 14 demonstrates that the percentages of positioning errors greater than 6 m for SSD-normal and PSSD-normal are 7.2% and 2.0%, respectively. However, the percentages are 10.3% and 7.0% for SSD-fast and PSSD-fast, respectively. Although the proposed PSSD can still achieve a reduction of large errors (>6 m in this case), the reduction from PSSD to SSD in fast mode (10.3% decreases slightly to 7.0%) is much less than that in normal mode (7.2% decreases sharply to 2.0%). This is because that fast walking mode widens the search of reference points (as shown by Figure 8), leading to a looser spatial constrain on the fingerprints. Nevertheless, we can still conclude that PSSD approach takes effect for both walking modes.

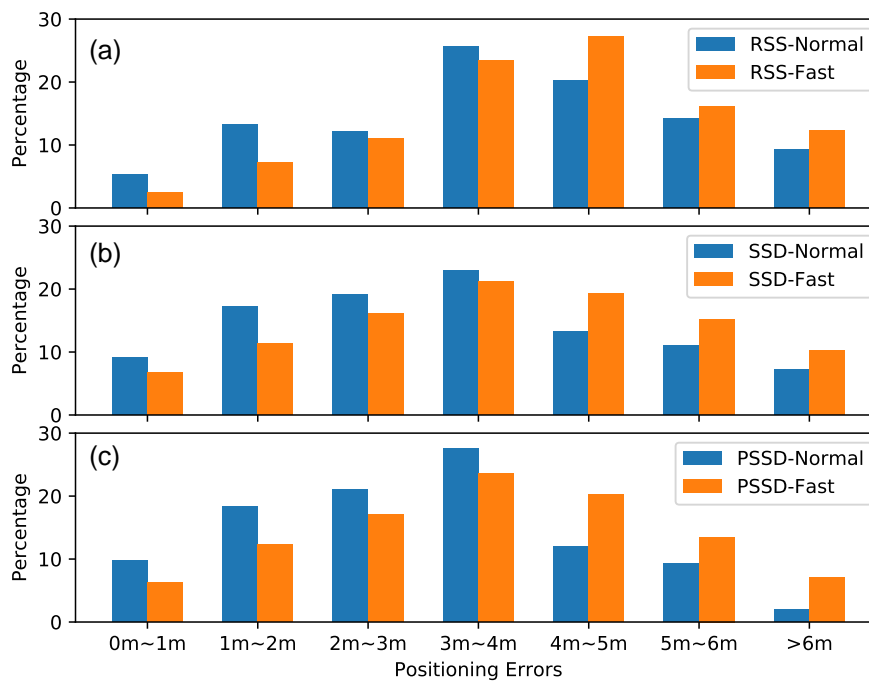


Figure 14. The probability distribution of positioning errors, denoting the walking speed influence on localization performance of given approach for heterogenous devices. The positioning errors have been classified into 7 levels: 0~1 m, 1~2 m, 2~3 m, 3~4 m, 4~5 m, 5~6 m and >6 m. (a), (b) and (c) denote the RSS, SSD and PSSD performances, respectively.)

5. Conclusions

In this study, we proposed the PSSD, a novel fingerprint-based smartphone indoor localization leveraging signals of opportunity of Wi-Fi RSS measurements. The proposed PSSD approach introduces three novel features for the fingerprinting method to improve usability: a newly defined vector of SSD observables, the spatial information of the pedestrian's mobility, and the pairwise RSS. The proposed PSSD method improves the usability of Wi-Fi RSS fingerprint positioning in two aspects. First, it mitigates the effect of the SSD among different smartphone devices, and the positioning performance is more consistent for different devices when a given fingerprint dataset is used. Second, with the proposed method, maximum errors decrease significantly, and the reliability of the positioning solution improves. With the newly defined SSD observables, the classic KNN algorithm in terms of the Pearson similarity metric is used in the online phase of the PSSD procedures. Compared to the legacy RSS fingerprinting methods, our experimental results suggest that the PSSD have few impacts for homogeneous devices; however, a significant average improvement of 20% in terms of positioning mean error was found for heterogeneous mobile devices. Thus, the proposed PSSD can enhance the usability of smartphone indoor positioning.

Considering the fact that the 90-percentile error of PSSD (~5 m) cannot currently fulfill the requirements of indoor positioning, we suggest some possible extensions of this work worthy of future research to further enhance the localization accuracy: (1) A particular treatment with the hidden error sources such as body-blocking and temporal environmental change may significantly reduce the positioning errors; (2) As a pure Wi-Fi fingerprinting method, our PSSD does not conflict with the conventional PDR/Wi-Fi fusion framework, and there should be an accuracy improvement if the PDR's distance/heading per step can be added to the fusion; (3) Another possible extension is to construct a longer time-series of RSS observations, i.e., modify the pairwise to the three-RSS form to constitute the RSS "historic track" that should better mitigate large positioning errors.

Author Contributions: Conceptualization, F.Y. and J.L.; Data curation, F.Y., C.W., Z.L. and P.T.; Formal analysis, F.Y. and J.L.; Funding acquisition, J.L. and R.C.; Methodology, F.Y. and J.L.; Resources, P.T.; Software, Z.L.; Supervision, J.X.; Validation, F.Y. and C.W.; Visualization, F.Y.; Writing—original draft, F.Y.; Writing—review and editing, J.X., J.L., C.W. and R.C.

Funding: This study was supported in part by the National Key Research Development Program of China with project No. 2016YFB0502204, National Natural Science Foundation of China (Grant No. 41804016 and Grant No. 41874031), the China Postdoctoral Science Foundation (Grant No. 2017M622517), the Technology Innovation Program of Hubei Province with Project No. 2018AAA070, and the Natural Science Fund of Hubei Province with Project No. 2018CFA007. This study was also Funded by State Key Laboratory of Geo-information Engineering, No. SKLGIE2017-M-1-1, and open foundation from State Key Laboratory of Geodesy and Earth's Geodynamics (Grant No. SKLGED2018-1-4-E).

Acknowledgments: Authors are grateful to the editor and three anonymous reviewers for their valuable comments, which we used to improve this study.

Conflicts of Interest: The authors declare no conflict of interest.

References

1. Global Indoor Location Market Analysis (2017–2023). Available online: <https://www.reportlinker.com/p05207399/Global-Indoor-Location-Market-Analysis.html> (accessed on 23 November 2017).
2. He, S.; Chan, S.H.G. Wi-Fi Fingerprint-Based Indoor Positioning: Recent Advances and Comparisons. *IEEE Commun. Surv. Tutor.* **2016**, *18*, 466–490. [[CrossRef](#)]
3. Basri, C.; Khadimi, A.E. Survey on indoor localization system and recent advances of WIFI fingerprinting technique. In Proceedings of the International Conference on Multimedia Computing and Systems, Marrakech, Morocco, 29 September–1 October 2016, pp. 253–259.
4. Correa, A.; Barcelo, M.; Morell, A.; Vicario, J.L. A Review of Pedestrian Indoor Positioning Systems for Mass Market Applications. *Sensors* **2017**, *17*, 1927. [[CrossRef](#)] [[PubMed](#)]
5. Zafari, F.; Gkelias, A.; Leung, K. A Survey of Indoor Localization Systems and Technologies. *arXiv* **2017**, arXiv:1709.01015.
6. Karaagac, A.; Haxhibeqiri, J.; Ridolfi, M.; Joseph, W.; Moerman, I.; Hoebeke, J. Evaluation of accurate indoor localization systems in industrial environments. In Proceedings of the IEEE International Conference on Emerging Technologies and Factory Automation, Limassol, Cyprus, 12–15 September 2017.
7. Martin, E.; Vinyals, O.; Friedland, G.; Bajcsy, R. Precise indoor localization using smart phones. In Proceedings of the International Conference on Multimedia 2010, Firenze, Italy, 25–29 October 2010; pp. 787–790.
8. Shu, Y.; Huang, Y.; Zhang, J.; Coué, P.; Cheng, P.; Chen, J.; Kang, G.S. Gradient-Based Fingerprinting for Indoor Localization and Tracking. *IEEE Trans. Ind. Electron.* **2016**, *63*, 2424–2433. [[CrossRef](#)]
9. Dortz, N.L.; Gain, F.; Zetterberg, P. WiFi fingerprint indoor positioning system using probability distribution comparison. In Proceedings of the IEEE International Conference on Acoustics, Speech and Signal Processing, Kyoto, Japan, 25–30 March 2012; pp. 2301–2304.
10. Ge, X.; Qu, Z. Optimization WIFI indoor positioning KNN algorithm location-based fingerprint. In Proceedings of the IEEE International Conference on Software Engineering and Service Science, Beijing, China, 26–28 August 2016; pp. 135–137.
11. Li, Z.; Liu, J.; Yang, F.; Niu, X.; Li, L.; Wang, Z.; Chen, R. A Bayesian Density Model Based Radio Signal Fingerprinting Positioning Method for Enhanced Usability. *Sensors* **2018**, *18*, 4063. [[CrossRef](#)] [[PubMed](#)]
12. Turner, D.; Savage, S.; Snoeren, A.C. On the empirical performance of self-calibrating WiFi location systems. In Proceedings of the Local Computer Networks, Bonn, Germany, 4–7 October 2011; pp. 76–84.
13. Hossain, A.K.M.M.; Jin, Y.; Soh, W.S.; Van, H.N. SSD: A Robust RF Location Fingerprint Addressing Mobile Devices' Heterogeneity. *IEEE Trans. Mob. Comput.* **2013**, *12*, 65–77. [[CrossRef](#)]
14. Haeberlen, A. Practical robust localization over large-scale 802.11 wireless networks. In Proceedings of the International Conference on Mobile Computing and Networking, Philadelphia, PA, USA, 26 September–1 October 2004; pp. 70–84.
15. Kjærsgaard, M.B. Automatic mitigation of sensor variations for signal strength based location systems. In Proceedings of the International Conference on Location- and Context-Awareness, Dublin, Ireland, 10–11 May 2006; pp. 30–47.

16. Wu, C.; Yang, Z.; Zhou, Z.; Liu, Y.; Liu, M. Mitigating Large Errors in WiFi-based Indoor Localization for Smartphones. *IEEE Trans. Veh. Technol.* **2017**, *66*, 6246–6257. [[CrossRef](#)]
17. Kim, Y.; Shin, H.; Cha, H. Smartphone-based Wi-Fi pedestrian-tracking system tolerating the RSS variance problem. In Proceedings of the IEEE International Conference on Pervasive Computing and Communications, Lugano, Switzerland, 19–23 March 2012; pp. 11–19.
18. Chen, Z.; Zou, H.; Jiang, H.; Zhu, Q.; Soh, Y.C.; Xie, L. Fusion of WiFi, smartphone sensors and landmarks using the Kalman filter for indoor localization. *Sensors* **2015**, *15*, 715–732. [[CrossRef](#)] [[PubMed](#)]
19. Liu, J.; Chen, R.; Ling, P.; Guinness, R.; Kuusniemi, H. A Hybrid Smartphone Indoor Positioning Solution for Mobile LBS. *Sensors* **2012**, *12*, 17208–17233. [[CrossRef](#)] [[PubMed](#)]
20. Tsui, A.W.; Chuang, Y.H.; Chu, H.H. Unsupervised Learning for Solving RSS Hardware Variance Problem in WiFi Localization. *Mob. Netw. Appl.* **2009**, *14*, 677–691. [[CrossRef](#)]
21. Han, S.; Zhao, C.; Meng, W.; Li, C. Cosine similarity based fingerprinting algorithm in WLAN indoor positioning against device diversity. In Proceedings of the IEEE International Conference on Communications, London, UK, 8–12 June 2015; pp. 2710–2714.
22. Xie, Y.; Wang, Y.; Nallanathan, A.; Wang, L. An Improved K-Nearest-Neighbor Indoor Localization Method Based on Spearman Distance. *IEEE Signal Process. Lett.* **2016**, *23*, 351–355. [[CrossRef](#)]
23. Wang, L.; Wu, X.; Zheng, B.; Cui, J.; Zhou, H. A cosine similarity-based compensation strategy for RSS detection variance in indoor localization. In Proceedings of the Telecommunication Networks and Applications Conference, Dunedin, New Zealand, 7–9 December 2017; pp. 47–52.
24. Dong, F.; Chen, Y.; Liu, J.; Ning, Q.; Piao, S. A Calibration-Free Localization Solution for Handling Signal Strength Variance. In Proceedings of the International Conference on Mobile Entity Localization and Tracking in GPS-Less Environments, Orlando, FL, USA, 30 September 2009.
25. Laoudias, C.; Piché, R.; Panayiotou, C.G. Device self-calibration in location systems using signal strength histograms. *J. Locat. Based Serv.* **2013**, *7*, 165–181. [[CrossRef](#)]
26. Liu, B.C.; Lin, K.H.; Wu, J.C. Analysis of hyperbolic and circular positioning algorithms using stationary signal-strength-difference measurements in wireless communications. *IEEE Trans. Veh. Technol.* **2006**, *55*, 499–509. [[CrossRef](#)]
27. Kjrgaard, M.B.; Munk, C.V. Hyperbolic Location Fingerprinting: A Calibration-Free Solution for Handling Differences in Signal Strength (concise contribution). In Proceedings of the IEEE International Conference on Pervasive Computing and Communications, Hong Kong, China, 17–21 March 2008; pp. 110–116.
28. Zheng, Z.; Chen, Y.; He, T.; Li, F.; Chen, D. Weight-RSS: A calibration-free and robust method for WLAN-Based indoor positioning. *Int. J. Distrib. Sens. Netw.* **2015**, *11*, 573582. [[CrossRef](#)]
29. Fang, S.H.; Wang, C.H.; Chiou, S.M.; Lin, P. Calibration-Free Approaches for Robust Wi-Fi Positioning against Device Diversity: A Performance Comparison. In Proceedings of the Vehicular Technology Conference, Yokohama, Japan, 6–9 May 2012; pp. 1–5.
30. Fet, N.; Handte, M.; Marrón, P.J. A model for WLAN signal attenuation of the human body. In Proceedings of the ACM International Joint Conference on Pervasive and Ubiquitous Computing, Zurich, Switzerland, 8–12 September 2013; pp. 499–508.
31. Li, X.; Wang, J.; Liu, C.; Zhang, L.; Li, Z. Integrated WiFi/PDR/Smartphone Using an Adaptive System Noise Extended Kalman Filter Algorithm for Indoor Localization. *ISPRS Int. J. Geo-Inf.* **2016**, *5*, 8. [[CrossRef](#)]
32. Chen, G.; Meng, X.; Wang, Y.; Zhang, Y.; Tian, P.; Yang, H. Integrated WiFi/PDR/Smartphone Using an Unscented Kalman Filter Algorithm for 3D Indoor Localization. *Sensors* **2015**, *15*, 24595–24614. [[CrossRef](#)] [[PubMed](#)]
33. Cho, H.; Kwon, Y. RSS-based indoor localization with PDR location tracking for wireless sensor networks. *AEUE Int. J. Electron. Commun.* **2016**, *70*, 250–256. [[CrossRef](#)]
34. Zhang, M.; Shen, W.; Yao, Z.; Zhu, J. Multiple information fusion indoor location algorithm based on WIFI and improved PDR. In Proceedings of the Chinese Control Conference, Chengdu, China, 27–29 July 2016; pp. 5086–5092.
35. Koo, B.; Lee, S.; Lee, M.; Lee, D.; Lee, S.; Kim, S. PDR/fingerprinting fusion indoor location tracking using RSS recovery and clustering. In Proceedings of the International Conference on Indoor Positioning and Indoor Navigation, Busan, South Korea, 27–30 October 2014; pp. 699–704.

36. Hassan, M. A performance model of pedestrian dead reckoning with activity-based location updates. In Proceedings of the IEEE International Conference on Networks, Singapore, 12–14 December 2012; pp. 64–69.
37. Radu, V.; Marina, M.K. HiMLoc: Indoor smartphone localization via activity aware Pedestrian Dead Reckoning with selective crowdsourced WiFi fingerprinting. In Proceedings of the International Conference on Indoor Positioning and Indoor Navigation, Montbeliard-Belfort, France, 28–31 October 2013; pp. 1–10.
38. Bahl, P.; Padmanabhan, V.N. RADAR: An In-Building RF-based User Location and Tracking System. In Proceedings of the INFOCOM 2000, Nineteenth Joint Conference of the IEEE Computer and Communications Societies, Tel Aviv, Israel, 26–30 March 2000; Volume 2, pp. 775–784.
39. Rappaport, T.S. *Wireless Communications: Principles and Practice*; Prentice-Hall, Inc.: Upper Saddle River, NJ, USA, 1995.
40. Saunders, S.R.; Simon, S.R. *Antennas and Propagation for Wireless Communication Systems*; J. Wiley and Sons, Inc.: New York, NY, USA, 1999; pp. 1–4.
41. Aitaterini, P.; Ji, T. Frequency and velocity of people walking. *Struct. Eng.* **2005**, *84*, 36–40.
42. Slater, J.A.; Malys, S. WGS 84—Past, Present and Future. In *Advances in Positioning and Reference Frames*; International Association of Geodesy Symposia; Brunner, F.K., Ed.; Springer: Berlin/Heidelberg, Germany, 1998; Volume 118.



© 2019 by the authors. Licensee MDPI, Basel, Switzerland. This article is an open access article distributed under the terms and conditions of the Creative Commons Attribution (CC BY) license (<http://creativecommons.org/licenses/by/4.0/>).